Appl. Phys. B 81, 963–968 (2005)
DOI: 10.1007/s00340-005-2019-7

Applied Physics B
Lasers and Optics

A.J. SCROGGIE
D. GOMILA
W.J. FIRTH
G.-L. OPPO✉

Spontaneous and induced motion of optical patterns

Department of Physics, University of Strathclyde, 107 Rottenrow, Glasgow G4 0NG, Scotland, UK

Received: 27 June 2005/Revised version: 31 August 2005
Published online: 4 November 2005 • © Springer-Verlag 2005

ABSTRACT The universality of two mechanisms of motion of patterns in nonlinear optics is demonstrated. In the first one, two-dimensional disordered patterns are shown to scroll with constant velocity after transients are discarded. In the second case, pattern motion is induced by background modulations. Spatially periodic patterns lock to maxima or minima of the underlying modulation depending on its wavevector.

PACS 42.65.Sf; 05.65.+b; 45.70.Qj

1 Introduction

Pattern formation in nonlinear optics has been described and observed in a variety of models and experimental realisations [1]. The intrinsic mechanism leading to regular spatial structures in the transverse plane of optical devices is the coupling of the optical nonlinearity with imaginary (diffraction) or real (diffusion) non-locality. Just above modulational instabilities of a homogeneous solution, patterns are in general stationary and a variety of geometries has been observed ranging from hexagons and rolls to honeycombs and squares. Patterned states are often an essential ingredient for the existence of localised structures that could find application in optical memories and information technologies. Control of size and geometry [2] of optical patterns is also possible, providing the operators with a variety of optical beams to tune to the desired application [3].

Away from modulational instabilities optical patterns may break up into dynamical structures of regular [4] or irregular shapes [5]. The onset of dynamical behaviour corresponds to instabilities of the stationary patterns often via Hopf or more complicated bifurcations. Spatio-temporal oscillations of patterns have recently been observed experimentally [6]. A large body of experimental evidence for moving patterns has also been reported in atomic [7] and photorefractive [8] media as well as in liquid crystal light valves [9].

Regular optical patterns can also move spontaneously, e.g. travelling waves in systems with phase invariance where the real and imaginary part of the fields are modulated but the total intensity is homogeneous [10]. These solutions are typical of laser systems where the optical gain is balanced by the cavity losses and have been observed recently in Vertical Cavity Surface Emitting Lasers (VCSELs) [11]. Another well-studied case of spontaneous uniform motion of a spatial structure is that of a Bloch wall in a non-equilibrium Ising–Bloch (NIB) transition [12, 13]. In this bifurcation a symmetric (Ising) front between two equivalent states becomes unstable to an asymmetric (Bloch) front. In non-variational systems the unstable mode of the Ising front is proportional to the neutral (Goldstone) mode and the wall moves [13]. This movement can be qualitatively understood as self-induced motion where the spatial structure induces a modulation, which, in turn, makes the spatial structure move. The neutral (gradient) mode of the wall couples to the unstable mode and induces a movement, which at the same time drags the unstable mode, self-sustaining the motion. A similar transition has also been noted in semiconductor devices, where thermal effects cause spontaneous motion of cavity solitons [14].

In this paper we analyse two cases of spontaneous and induced motion of optical patterns that have not yet been studied in their own right. First of all, we describe in Sect. 2 the 'scrolling' motion of disordered patterns in two dimensions (2D). This dynamical behaviour is similar to a travelling wave but with no pre-assigned direction of motion. Scrolling motion has been observed in numerical simulations since the early 1990s and we demonstrate its universality in optics. We also provide a numerical method for the prediction of its (constant) velocity. The second case, analysed in Sect. 3, corresponds to the motion of regular patterns induced by the presence of a modulated background. As for cavity solitons in the presence of modulated parameters [15], patterns may move towards and remain locked to either maxima or minima of the modulations depending on the magnitude of the background wavevector. Conclusions and future developments are discussed in Sect. 4.

2 Spontaneous motion of 2D disordered patterns

In this section we present evidence of spontaneous motion of disordered 2D patterns. In spite of the irregular nature of the spatial structures, their velocity is constant in magnitude and direction and the motion can intuitively be described as 'scrolling'. This movement is not associated with

✉ Fax: 00-44-141-552-2891, E-mail: g.l.oppo@phys.strath.ac.uk

a 'NIB-like' transition and the asymmetry of the pattern is not related to any bifurcation. This phenomenon was first observed by Oppo et al. in a degenerate optical parametric oscillator (DOPO) [17], where the movement of a stripe pattern with defects due to a zigzag instability was reported. Here we show that such motion is universal and is present in disordered patterns in several types of nonlinear optical systems.

We first present the scrolling motion of a disordered roll pattern in the singly resonant DOPO (SRDOPO). A phase-matched SRDOPO, where there is no cavity for the pump field, can be described in the mean-field approximation by [16]

$$\partial_t A = -A - \mathrm{i}\Delta A + EA^* - |A|^2 A + \mathrm{i}\nabla^2 A\,, \tag{1}$$

where $A(x, y, t)$ is the slowly varying amplitude of the signal, Δ is the cavity detuning, E is the amplitude of the external pump field, and $\nabla^2 = \partial_x^2 + \partial_y^2$ is the transverse Laplacian. The homogeneous solution $A = 0$ is stable for $E < 1$. At threshold, a ring of unstable wavevectors with modulus $k_c = \sqrt{-\Delta}$ becomes unstable. Above, but close to, threshold, nonlinear competition leads to the selection of a perfect stationary stripe pattern [18]. If one suddenly sets the system well above threshold, however, disordered patterns consisting of portions of stripe patterns of different orientations are obtained. After a transient such patterns reach a frozen state and, typically, a slow scrolling motion is observed (Fig. 1). The velocity of the global motion is finite for all values of the parameters where a particular pattern exists, and the direction of motion is constant. Figure 1 shows the modulus of the velocity $v = \sqrt{v_x^2 + v_y^2}$ as a function of the control parameter for a particular disordered stripe pattern. This solution was obtained from a numerical simulation of (1) starting from a random initial condition 30% above threshold ($E = 1.3$). Then, we determine the solution and its velocity for different values of the control parameter by solving

$$-A - \mathrm{i}\Delta A + EA^* - |A|^2 A + \mathrm{i}\nabla^2 A - v_x \partial_x A - v_y \partial_y A = 0 \tag{2}$$

using a Newton method. In addition to (2), two extra equations to determine the two components of the velocity v_x and v_y are needed. We use the integral phase conditions [19]

$$\int A\,\partial_x A_0\,\mathrm{d}x = 0\,,$$
$$\int A\,\partial_y A_0\,\mathrm{d}y = 0\,, \tag{3}$$

where $A_0(x, y)$ is a reference solution, which we take to be the solution obtained at each previous value of the control parameter during continuation. Equations (3) fix the position of the solution, which with periodic boundary conditions is undetermined, imposing that the solution for the new value of the parameter is at the same position as the reference solution A_0. This provides two extra equations independent of the other N^2 given by (2), where N is the number of grid points (typically $N = 32$).

The inset in Fig. 1 shows the actual motion of the structure from a numerical simulation for $E = 1.3$. The arrow on the right shows the direction of the motion. In the same parameter region, this solution co-exists with many other possible disordered states as well as stationary regular patterns. Figure 2 shows an example of a perfect stripe pattern. Different disordered patterns move, in general, in different directions and at different speeds. Figures 3 and 4 show examples of scrolling motion of other disordered patterns. The direction and magnitude of the velocity depend on the specific features of the profile of the disordered pattern. Such features change

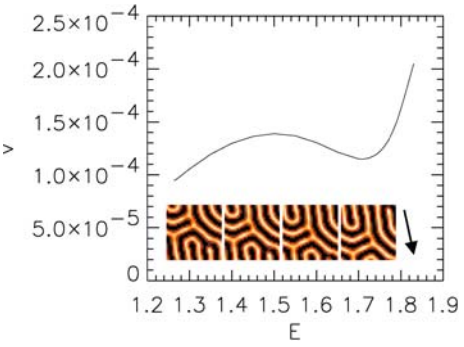

FIGURE 1 Scrolling velocity of a disordered stripe pattern as a function of the control parameter E in the SRDOPO for $\Delta = -1$. The *inset* shows the scrolling motion of $\mathrm{Re}(A)$ from a numerical simulation for $E = 1.3$. We integrate (1) using a pseudospectral method where linear terms are treated exactly in Fourier space while a second order in time approximation is used for the nonlinear terms. The integration in Fourier space automatically imposes periodic boundary conditions. The size of the system is $L = 32$. The *arrow* on the *right* indicates the direction of the scrolling motion

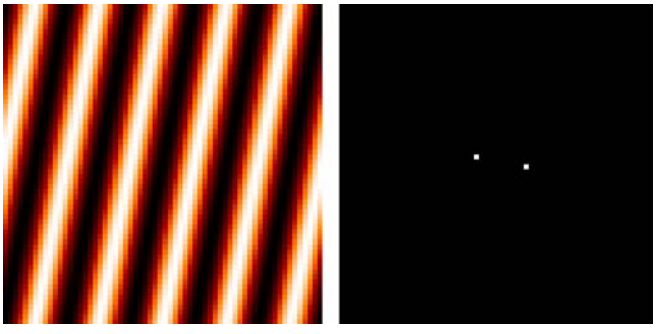

FIGURE 2 Real part ($\mathrm{Re}(A(x, y))$) of the electric field (*left*) and power spectrum ($|A(k_x, k_y)|^2$) (*right*) of a regular stripe pattern obtained in the SRDOPO by increasing the pump adiabatically from below threshold up to $E = 1.3$. All other parameters are as in Fig. 1. *Darker colours* indicate lower values

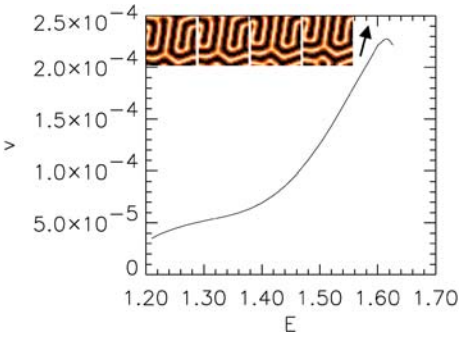

FIGURE 3 The same as in Fig. 1 but for a different SRDOPO disordered pattern obtained by changing the initial condition

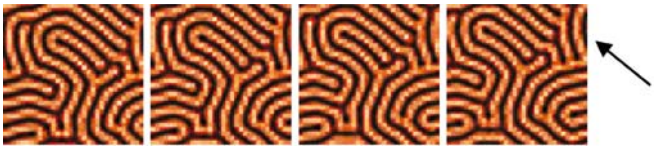

FIGURE 4 Scrolling disordered stripe pattern obtained from a numerical simulation of (1) starting from a random initial condition in a larger system. All the parameters are as in Fig. 1 and the size of the system has been doubled. The *arrow* on the *right* indicates the direction of the motion. In this case the modulus of the velocity is 1×10^{-4}

in a non-trivial way with the control parameters and, for example, the velocity shows a non-monotonic dependence on the input pump E of the SRDOPO as shown in Figs. 1 and 3 for two co-existing disordered patterns. Secondary bifurcations of these patterned solutions also affect the scrolling velocity, but this is left to a future investigation.

Another example of scrolling motion can be observed in labyrinthine patterns. This kind of structure is formed when a front between two equivalent states becomes modulationally unstable [20]. A prototypical model to study this phenomenon is the parametrically driven complex Ginzburg–Landau (PCGL) equation, which is the generic amplitude equation for an oscillatory system parametrically forced at twice its natural frequency:

$$\partial_t A = (1+\mathrm{i}\alpha)\nabla^2 A + (\mu+\mathrm{i}\nu)A - (1+\mathrm{i}\beta)|A|^2 A + pA^*\,, \tag{4}$$

where α is the ratio between diffraction and diffusion, μ measures the distance from the oscillatory instability threshold, ν is the detuning, and $p > 0$ is the forcing amplitude. For $p > p_\mathrm{h}$ large enough, (4) presents two equivalent homogeneous solutions, and for $p_\mathrm{h} < p < p_\mathrm{c}$ a front connecting these two solutions is modulationally unstable leading to the formation of labyrinthine patterns. Figure 5 shows the scrolling velocity for such a pattern obtained as explained above. The symbols show, for comparison, the results obtained by evaluating the velocity from numerical simulations of (4), in very good agreement with the exact results obtained from the Newton method. We note that these results are obtained in a parameter region far away from any NIB transition where

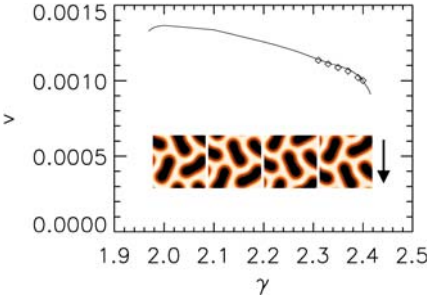

FIGURE 5 Velocity of the scrolling motion of a labyrinthine pattern as a function of the control parameter γ in the PCGL. Here $\alpha = 2$, $\beta = 0$, $\nu = 2$, and $\mu = 0$. For these values of the parameters $p_\mathrm{h} = 2.06$ and $p_\mathrm{c} = 2.57$. The *solid line* shows the value of the velocity obtained with a Newton method, while the *symbols* show the results obtained from numerical simulations. The *inset* shows $\mathrm{Re}(A)$ from a numerical simulation for $\gamma = 2.31$. The *arrow* on the *right* shows the direction of the scrolling motion

only symmetric Ising walls exist, and therefore the motion cannot be associated with the motion of asymmetric Bloch walls, but it is an intrinsic property of such disordered structures. We observe scrolling motion for any parameter values where the labyrinthine pattern exists and expect similar behaviour for any system where such disordered patterns are formed.

The modulus and direction of the velocity depend on the specific features of the spatial profile of the disordered patterns. The velocity does not depend explicitly on the size of the system but, in general, disordered solutions tend to scroll more slowly in systems with broad transverse section. The reason is that in broad-area systems, an irregular pattern can be interpreted as formed by different sub-regions that in a smaller system would move in different directions and that average out the total scrolling motion of the pattern. The detailed scaling properties of the velocity as a function of the system size will be analysed elsewhere.

3 Induced motion of optical patterns

In this section we consider dissipative nonlinear systems which are translationally invariant, and which possess a spatially varying, time-independent solution $E_0(x)$. A small perturbation ΔP which breaks the translational invariance generally induces motion of the solution, with a velocity given by [21]

$$v(x) = -\frac{\langle\psi_0|\Delta P\rangle}{\langle\psi_0|\phi_0\rangle}\,. \tag{5}$$

Here ϕ_0 and ψ_0 are, respectively, the null eigenfunctions of the Jacobian of the system and its adjoint, evaluated at E_0 when $\Delta P = 0$.

Cosinusoidal modulations ($\Delta P \propto \cos(Kx)$) form an interesting and fundamentally important class of perturbations. In that case, if the spatial structure is an even function of x, the velocity can be written in the form [15]

$$v(x) = A(K)\sin(Kx)\,. \tag{6}$$

The function $A(K)$ is odd, and depends on the structure of E_0 and on the nature of the coupling between the perturbation and the fields (e.g. amplitude or phase modulation). Previously [15] we have shown that for spatial soliton solutions, $A(K)$ generally undergoes changes of sign as K is varied. This means that a soliton can ascend or descend a modulation gradient, depending on the wavevector of the modulation. Zeros of $A(K)$ imply no motion of the soliton at any point in space, despite the existence of the modulation. In the remainder of this section we extend the analysis to cover periodic patterns.

We examine the response of one-dimensional roll patterns to a cosinusoidal modulation in one of the system parameters. As a concrete example, we consider the mean-field model of a two-level medium in an optical cavity [22]:

$$\partial_t E = -(1+\mathrm{i}\theta)E + P - \frac{2C(1-\mathrm{i}\Delta)}{1+\Delta^2+|E|^2}E + \mathrm{i}\partial_{xx}E\,. \tag{7}$$

The terms on the right-hand side represent, in order, reflection losses at the mirrors, cavity detuning, the external driving

field, the absorptive and dispersive effects of the two-level medium, and diffraction. The parameter θ is the detuning between the intra-cavity field E and the nearest cavity resonance, Δ is the difference between the frequency of the driving field and the resonant frequency of the atomic transition, and $2C$ is the coupling constant between the material and the intracavity field. The time has been scaled to the cavity lifetime.

Equation (7) can form a pattern (roll) solution E_0, with wavevector K_0, when a spatially homogeneous pump field P drives the system above its modulational instability threshold [22]:

$$E_0 = \sum_{n=0}^{\infty} a_n \cos(nK_0 x)\,. \tag{8}$$

Here, instead, we consider pump fields of the form

$$\begin{aligned} P &= P_0(1+\mu_{\mathrm{R}}\sin(Kx+\phi))\mathrm{e}^{\mathrm{i}\mu_{\mathrm{I}}\sin(Kx+\phi)} \\ &\simeq P_0(1+\mu\sin(Kx+\phi)) \\ &= P_0 + \Delta P\,, \end{aligned} \tag{9}$$

where $K = mK_0$, $\mu \equiv \mu_{\mathrm{R}} + \mathrm{i}\mu_{\mathrm{I}}$, and $|\mu| \ll 1$. Without loss of generality, P_0 is assumed to be real. We only consider cases where m is rational, so that K and K_0 are commensurate. In fact, initially we consider m to be an integer so that the modulation frequency is already present in the pattern.

The modulation induces motion and, to lowest order in $|\mu|$, the velocity is given by (5). From (8), the functions ϕ_0 and ψ_0 have the form

$$\phi_0 = \sum_{n=1}^{\infty} f_n \sin(nK_0 x)\,, \quad \psi_0 = \sum_{n=1}^{\infty} g_n \sin(nK_0 x) \tag{10}$$

or, using 1 and i as a basis,

$$\begin{aligned} \phi_0 &= \begin{bmatrix} \sum_{n=1}^{\infty} \mathrm{Re}(f_n)\sin(nK_0x) \\ \sum_{n=1}^{\infty} \mathrm{Im}(f_n)\sin(nK_0x) \end{bmatrix}, \\ \psi_0 &= \begin{bmatrix} \sum_{n=1}^{\infty} \mathrm{Re}(g_n)\sin(nK_0x) \\ \sum_{n=1}^{\infty} \mathrm{Im}(g_n)\sin(nK_0x) \end{bmatrix}. \end{aligned} \tag{11}$$

In this basis

$$\Delta P = \begin{bmatrix} \mu_{\mathrm{R}} P_0 \sin(mK_0x+\phi) \\ \mu_{\mathrm{I}} P_0 \sin(mK_0x+\phi) \end{bmatrix}, \tag{12}$$

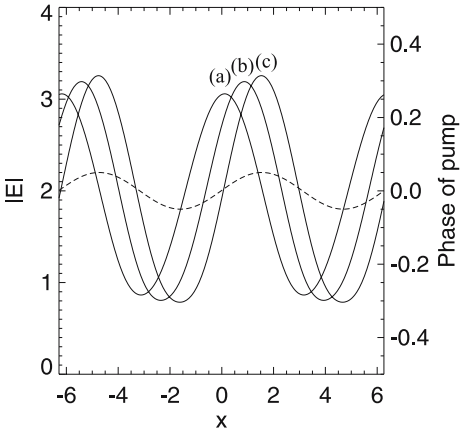

FIGURE 7 Time sequence of a pattern ascending the gradient of a phase-modulated pump. The modulation wavevector matches that of the pattern. (a) $t = 0$, (b) $t = 10$, and (c) $t = 50$ cavity lifetimes. $\mu = 0.05\mathrm{i}$; other parameters as in Fig. 6. The *dashed line* shows the phase of the pump

so that

$$v(x) \propto P_0 \cos(\phi(x))(\mu_{\mathrm{R}}\,\mathrm{Re}(g_m) + \mu_{\mathrm{I}}\,\mathrm{Im}(g_m))\,, \tag{13}$$

where (cf. (9)) $\phi(x)$ denotes the relative phase of the modulation and the pattern. If, for example, the pump is phase modulated ($\mu_{\mathrm{R}} = 0$), and $\mathrm{Im}(g_{m1})$ and $\mathrm{Im}(g_{m2})$ have different signs, then a peak of the pattern should move up the phase gradient for one value of m, and move down it for the other: the motion will reverse.

Figure 6 shows the real and imaginary parts of a section of the spectrum of ψ_0 for a typical pattern. Changes of sign are apparent (more so in the real part) between the second and third, and third and fourth, harmonics, indicating reversal of motion. Figures 7 and 8 show time sequences for $m = 2$ and $m = 3$ demonstrating that in the former case a peak of the pattern ascends the phase gradient, while in the latter case it descends, confirming the analysis. The simulations also indicate no reversal of motion between $m = 1$ and $m = 2$, and another reversal between $m = 3$ and $m = 4$, all in agreement with Fig. 6.

In general the $\{g_n\}$ do not have the same phase. Nevertheless, in this case at least, a change of sign in $\mathrm{Im}(g_n)$ is accompanied by a change of sign in $\mathrm{Re}(g_n)$. This implies that reversal of motion will occur at the same modulation frequen-

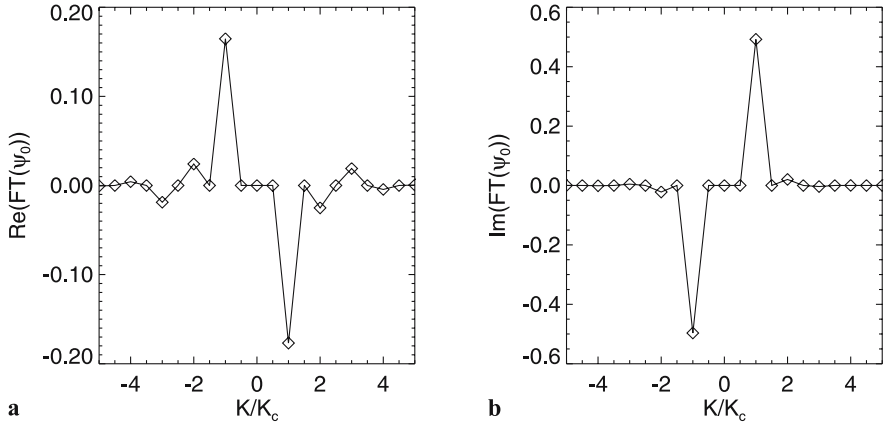

FIGURE 6 Section of Fourier spectrum of ψ_0 for a roll pattern in the two-level system. $\Delta = 0$, $\theta = -1$, $C = 5$, $P_0 = 6.3$ (and $\mu = 0$)

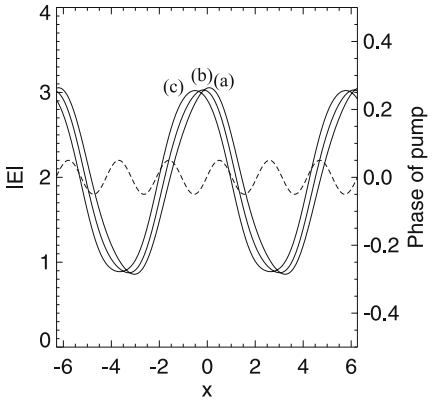

FIGURE 8 Time sequence of a pattern descending the gradient of a phase-modulated pump. The modulation wavevector is three times that of the pattern. (a) $t = 0$, (b) $t = 25$, and (c) $t = 100$ cavity lifetimes. $\mu = 0.05$i; other parameters as in Fig. 6. The *dashed line* shows the phase of the pump

cies regardless of the phase of μ. Simulations confirm that reversals occur at the same frequencies for both amplitude- and phase-modulated pumps.

If the modulation is not a harmonic of the pattern (m still rational but not an integer), (5) would imply that the velocity is zero, although this would only be true to lowest order. By definition, some harmonic of the phase modulation will match another (possibly high) harmonic of the pattern, so there will be some weak coupling between the perturbation and the translational mode of the pattern. This is a moot point, however, because a more significant effect is that the pattern is forced at the modulation frequency, resulting in minor or major distortions (see Fig. 9 for an amplitude-modulated pump). The effect is more pronounced for smaller modulation wavevectors, where the system response is greater, and rapidly tails off as the modulation wavevector increases.

We can replace the two-level medium in (7) with a self-focussing Kerr medium

$$\partial_t E = -(1 + \mathrm{i}\theta)E + P + \mathrm{i}|E|^2 E + \mathrm{i}\partial_{xx} E\,. \tag{14}$$

Equation (14) also possesses a modulational instability when P is a plane wave [23]. For a typical roll pattern in this system, we observe no changes of sign in the first few components g_n of ψ_0 (Fig. 10) and no reversal of motion in the simulations. Note that although (7) and (14) are quite similar, the simulations presented in the previous figures are obtained for

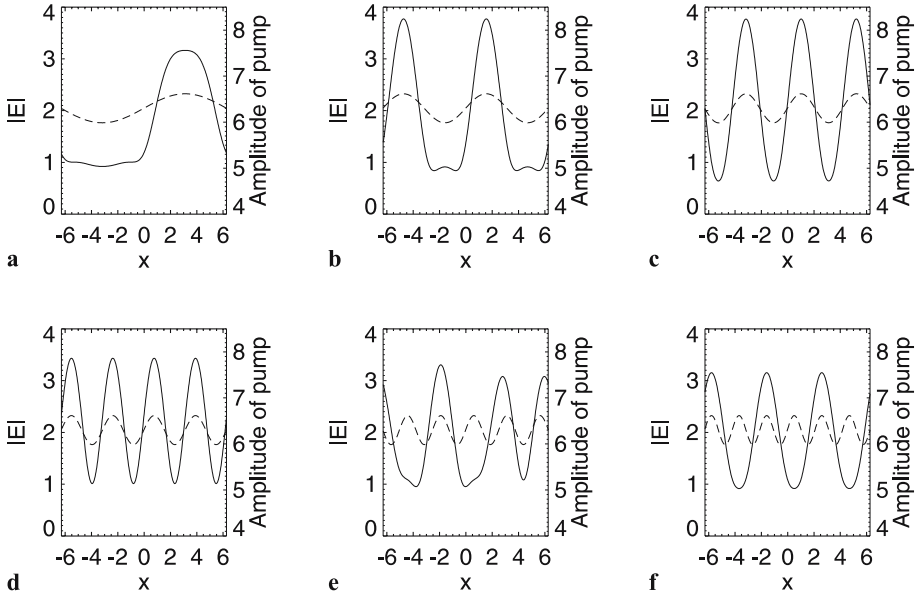

FIGURE 9 Forcing of pattern by amplitude-modulated pump ($\mu = 0.05$). (**a**) $m = 1/3$, (**b**) $m = 2/3$, (**c**) $m = 1$, (**d**) $m = 4/3$, (**e**) $m = 5/3$, (**f**) $m = 2$. In all cases the initial condition is the same pattern solution, computed at $\mu = 0$, whose period is one-third of the domain width. All other parameters as in Fig. 6. The *dashed line* shows the amplitude of the pump

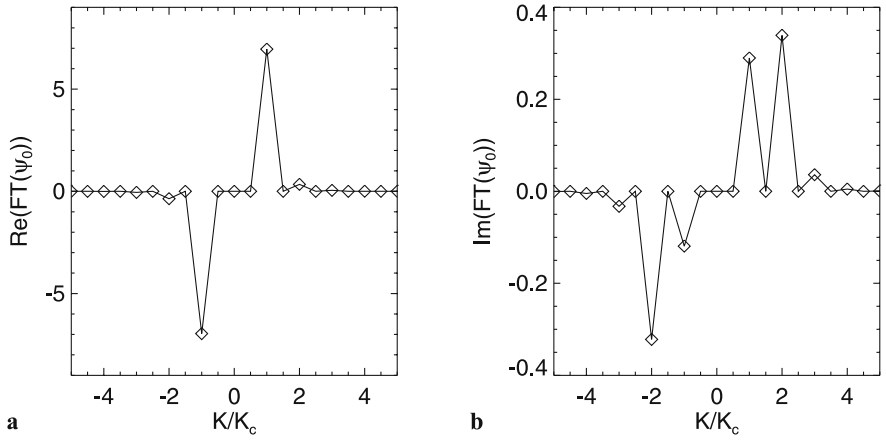

FIGURE 10 Section of Fourier spectrum of ψ_0 for a roll pattern in the Kerr cavity system. $\theta = 0$, $P_0 = 1.559$ (and $\mu = 0$). The spectrum is slightly asymmetric because the centre of the pattern lies between two grid points

the two-level saturable absorber with $\Delta = 0$, corresponding to a real nonlinearity, while the Kerr case has a purely imaginary one. By expanding the nonlinear term of (7) for large $|\Delta|$ and small E, one recovers the Kerr nonlinearity from that of the two-level saturable absorber. The disappearance of the reversal of motion of the pattern can be observed on progressively increasing the parameter $|\Delta|$ in a way similar to the observed disappearance of the reversal of motion of a cavity soliton in a modulated DOPO on increasing the input pump parameter (see Ref. [15] for details).

4 Conclusions and acknowledgements

Two examples of spontaneous and induced motion of patterns have been discussed. Spontaneous scrolling motion of 2D disordered structures is a universal feature of pattern-forming systems and is characterised by a constant velocity after transients have been discarded. In the case of induced motion, we showed that regular patterns may move towards maxima or minima of a background modulation depending on its wavevector.

The scrolling motion in 2D is due to the presence of asymmetry of the disordered structure and periodic boundary conditions. The scaling of the velocity and duration of the transient under coarse-graining transformations is under investigation.

When the motion of patterns is induced by modulations of the input pump at harmonics of the spatially periodic structure, the pattern moves rigidly in a direction determined by the input wavevector. For non-harmonic modulations, patterns deform locally to adjust their shape to the background. Spectral analysis of the deformed pattern should reveal the spatial modes that are preferred under these modifications and is the subject of new investigations.

We acknowledge support from the European projects QUANTIM and FunFACS and from EPSRC. AJS and GLO acknowledge support from SGI. GLO thanks the Royal Society–Leverhulme Trust and Centro Studi Dinamiche Complesse, University of Florence, Sesto Fiorentino, Italy.

We dedicate this contribution to Prof. Wulf Lange, a pioneering and inspirational figure in the field of complex optical structures.

REFERENCES

1 See the special issues by L.A. Lugiato (ed) Chaos, Noise Fractals **4** (1994), R. Neubecker (ed) Chaos, Noise Fractals **10** (1999), and M. Haelterman, R. Vilaseca (eds) J. Opt. B: Quantum S. O. **6** (2004)
2 R. Martin, A.J. Scroggie, G.-L. Oppo, W.J. Firth, Phys. Rev. Lett. **77**, 4007 (1996)
3 G.K. Harkness, G.-L. Oppo, W.J. Firth, Opt. Photonics News **9**, 44 (1998)
4 D. Gomila, P. Colet, Phys. Rev. A **68**, 011 801(R) (2003)
5 G. D'Alessandro, W.J. Firth, Phys. Rev. A **46**, 537 (1992)
6 S. Residori, A. Petrossian, L. Gil, Phys. Rev. Lett. **88**, 233 901 (2002)
7 See for example A. Aumann, T. Ackemann, E. Grosse Westhoff, W. Lange, Int. J. Bifurcat. Chaos **11**, 2789 (2001). For a review see T. Ackemann, W. Lange, Appl. Phys. B **72**, 21 (2001)
8 See for example Z. Chen, D. McGee, N.B. Abraham, J. Opt. Soc. Am. B **13**, 1482 (1996). For a review see C. Denz, M. Schwab, C. Weilnau, *Transverse Pattern Formation in Photorefractive Optics* (Springer Tracts Phys. **188**) (Springer, Berlin 2004)
9 See for example E. Benkler, M. Kreuzer, R. Neubecker, T. Tschudi, Phys. Rev. Lett. **84**, 879 (2000). For a review see F.T. Arecchi, S. Ducci, E. Pampaloni, P.L. Ramazza, S. Residori, J. Nonlinear Opt. Phys. Mater. **9**, 183 (2000)
10 P.K. Jakobsen, J. Lega, Q. Feng, M. Staley, J.V. Moloney, A.C. Newell, Phys. Rev. A **49**, 4189 (1994); J. Lega, P.K. Jakobsen, J.V. Moloney, A.C. Newell, Phys. Rev. A **49**, 4201 (1994); G.K. Harkness, W.J. Firth, J.B. Geddes, J.V. Moloney, E.M. Wright, Phys. Rev. A **50**, 4310 (1994)
11 S.P. Hegarty, G. Huyet, J.G. McInerney, K.D. Choquette, Phys. Rev. Lett. **82**, 1434 (1999)
12 P. Coullet, J. Lega, B. Houchmanzadeh, J. Lajzerowicz, Phys. Rev. Lett. **65**, 1352 (1990); P. Coullet, K. Emilsson, Physica D **61**, 119 (1992)
13 D. Michaelis, U. Peschel, F. Lederer, D.V. Skryabin, W.J. Firth, Phys. Rev. E **63**, 066 602 (2001)
14 A.J. Scroggie, J.M. McSloy, W.J. Firth, Phys. Rev. E **66**, 036 610 (2002)
15 A.J. Scroggie, J. Jeffers, G. McCartney, G.-L. Oppo, Phys. Rev. E **71**, 046 602 (2005)
16 S. Longhi, J. Mod. Optic. **43**, 1089 (1996); G.-L. Oppo, A.J. Scroggie, W.J. Firth, Phys. Rev. E **63**, 066 209 (2001)
17 G.-L. Oppo, M. Brambilla, L.A. Lugiato, Phys. Rev. A **49**, 2028 (1994)
18 M.A. Vorontsov, W.J. Firth, Phys. Rev. A **49**, 2891 (1994)
19 Y.A. Kuznetsov, *Elements of Applied Bifurcation Theory*, 2nd edn. (Springer, New York 1998)
20 D. Gomila, P. Colet, G.-L. Oppo, M. San Miguel, Phys. Rev. Lett. **87**, 194 101 (2001); D. Gomila, P. Colet, M. San Miguel, A.J. Scroggie, G.-L. Oppo, J. Quantum Electron. **39**, 238 (2003); D. Gomila, P. Colet, G.-L. Oppo, M. San Miguel, J. Opt. B **6**, S265 (2004)
21 T. Maggipinto, M. Brambilla, G.K. Harkness, W.J. Firth, Phys. Rev. E **62**, 8726 (2000)
22 L.A. Lugiato, C. Oldano, Phys. Rev. A **37**, 3896 (1988); W.J. Firth, A.J. Scroggie, Europhys. Lett. **26**, 521 (1994)
23 L.A. Lugiato, R. Lefever, Phys. Rev. Lett. **58**, 2209 (1987)